Electronic Supplementary Material (ESI) for Nanoscale.

Supporting Information

Highly Efficient Copper Halide Scintillators for High-Performance and Dynamic X-ray Imaging

Quan Zhou, Jiwei Ren, Jiawen Xiao, Lin Lei, Feiyi Liao, Haipeng Di, Chao Wang, Lijun Yang, Qi Chen, Xiaofang Yang, Yiying Zhao*, Xiaodong Han**

Q. Zhou, J. Ren, Dr. L. Lei, Dr. F. Liao, H. Di, L. Yang, Prof. Y. Zhao
Institute of Materials
China Academy of Engineering Physics
Jiangyou 621908, China
E-mail: zhaoyiying@caep.cn

Q. Zhou, Prof. J. Xiao, C. Wang, Prof. X. Han
Institute of Microstructure and Property of Advanced Materials, Beijing Key Lab of Microstructure and Property of Advanced Materials, faculty of materials and manufacturing
Beijing University of Technology
Beijing 100124, China
E-mail: xiaojw@bjut.edu.cn; xdhan@bjut.edu.cn

Prof. Q. Chen
School of Materials Science & Engineering
Beijing Institute of Technology
Beijing 100081, China

Prof. X. Yang
College of Materials Science and Engineering
Chongqing University
Chongqing 400044, China

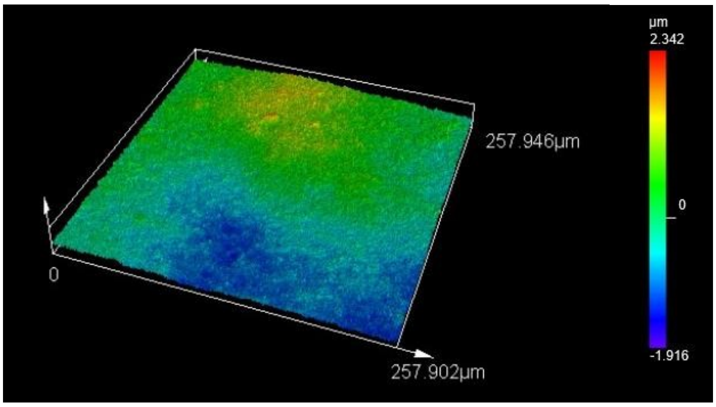

Figure S1. 3D image of the drop-casted β-$Cs_3Cu_2Cl_5$ film generated by a laser scanning confocal microscope.

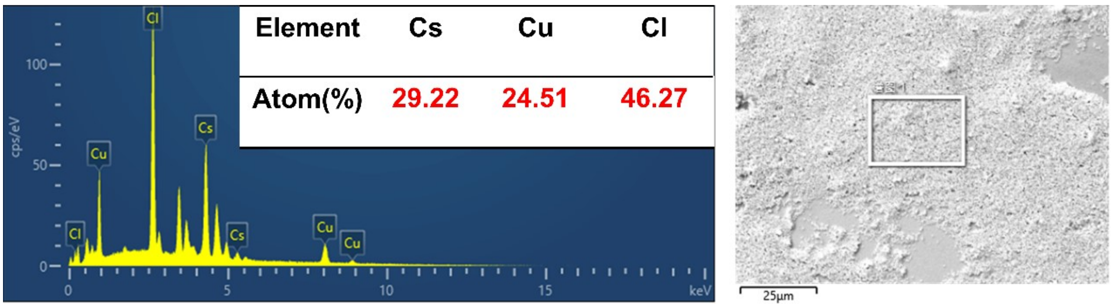

Figure S2. EDS elemental analysis of β-$Cs_3Cu_2Cl_5$ film.

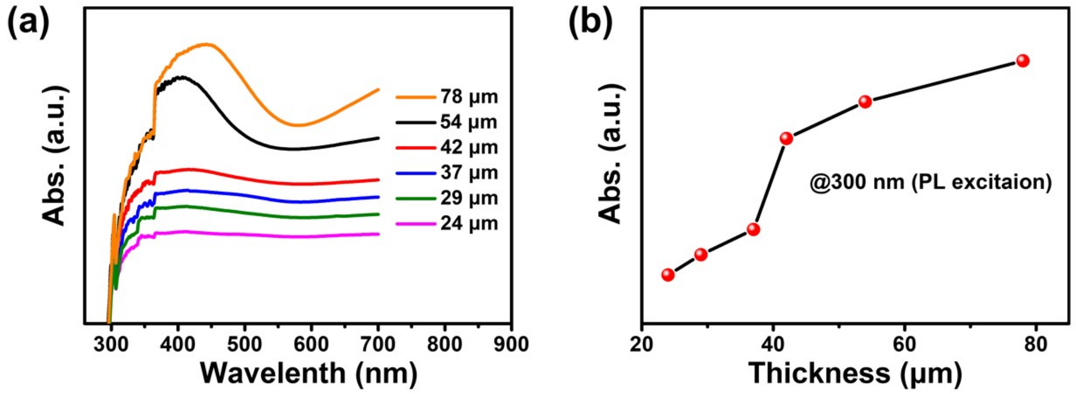

Figure S3. (a) UV-vis absorption spectra of films with varied thickness **(b)** Absorbance value at 300 nm of series films with varied thickness.

Due to the measurement limits of the UV-Vis absorption spectrometer, we cannot obtain the absorption spectra of films thicker than 80 um. The absorption data with varied thickness (smaller than 80 um) were provided, as shown in **Figure S3**. The increased baseline in the absorption spectra shown in the left figure is mainly caused by the enhanced light scattering from the increased surface roughness (**Figure S4**). The absorption at 300 nm of β-Cs3Cu2Cl5 films increases with the increased film thickness (no thicker than 80 um), as shown in **Figure S3(b)**, indicating that the corresponding enhanced PL intensity in **Figure 2b**.

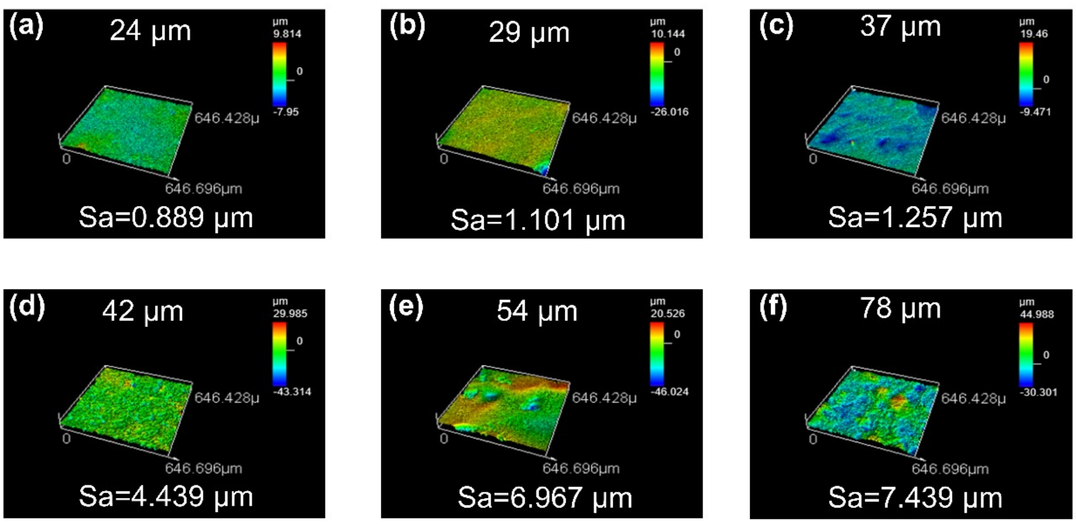

Figure S4. Surface roughness of β-$Cs_3Cu_2Cl_5$ films in varied thickness.

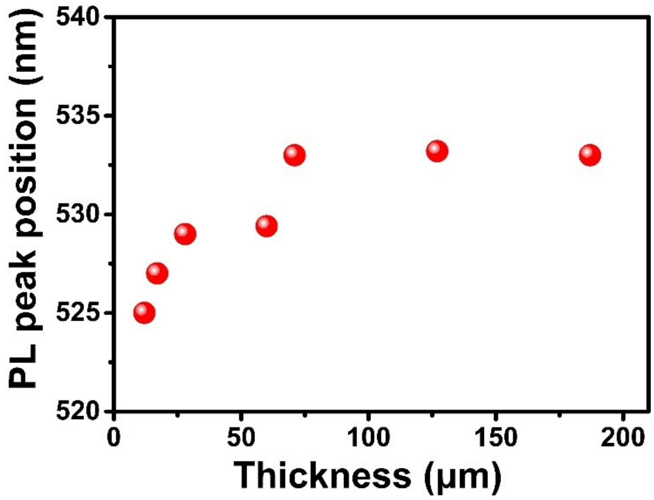

Figure S5. PL spectra peak positions of the β-$Cs_3Cu_2Cl_5$ films in different thickness.

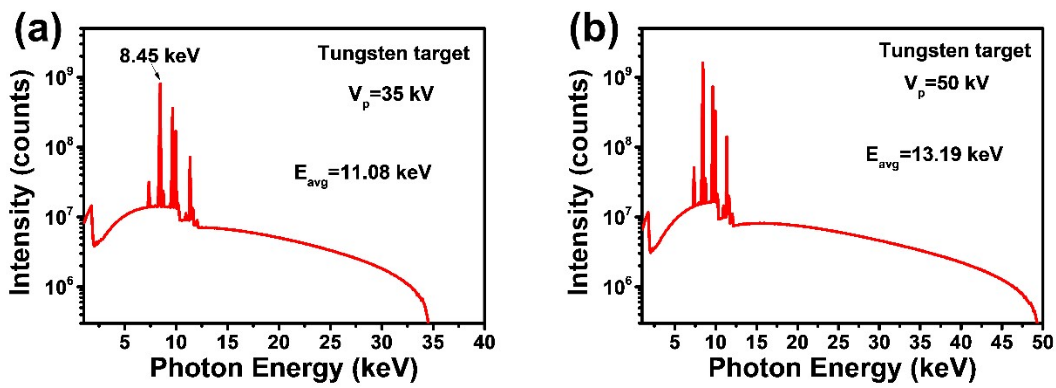

Figure S6. X-ray photon energy spectra generated by tungsten target at accelerating voltage of **(a)** 35 kV and **(b)** 50 kV.

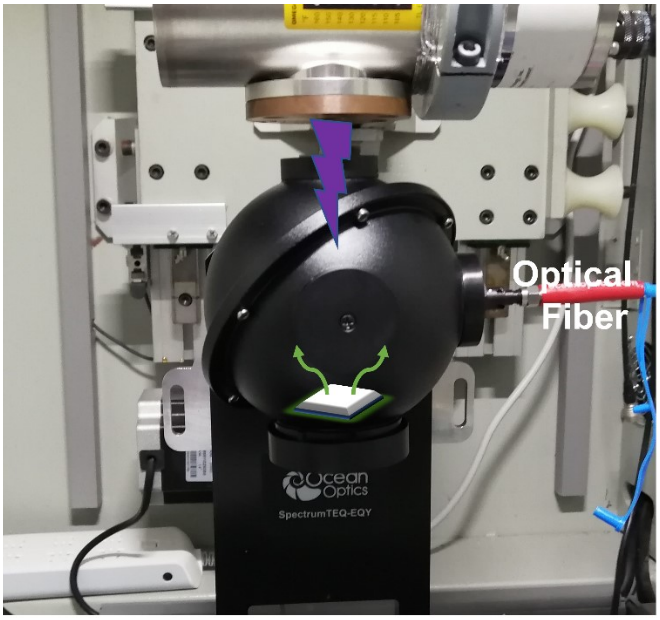

Figure S7. Photograph of the radioluminescence (RL) measurement system.

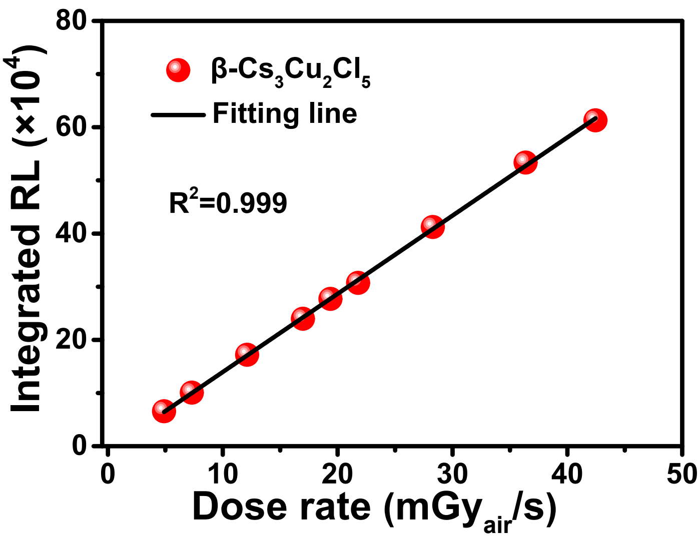

Figure S8. Linear relationship between integrated RL intensity of the β-$Cs_3Cu_2Cl_5$ films and X-ray dose rate.

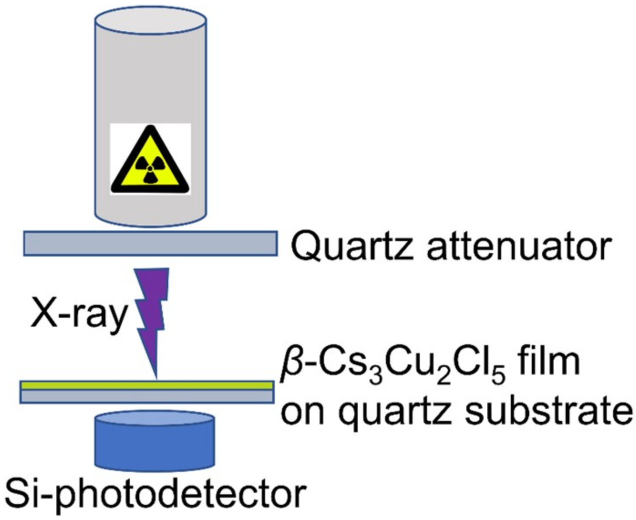

Figure S9. Schematic illustration of RL light power measurement system.

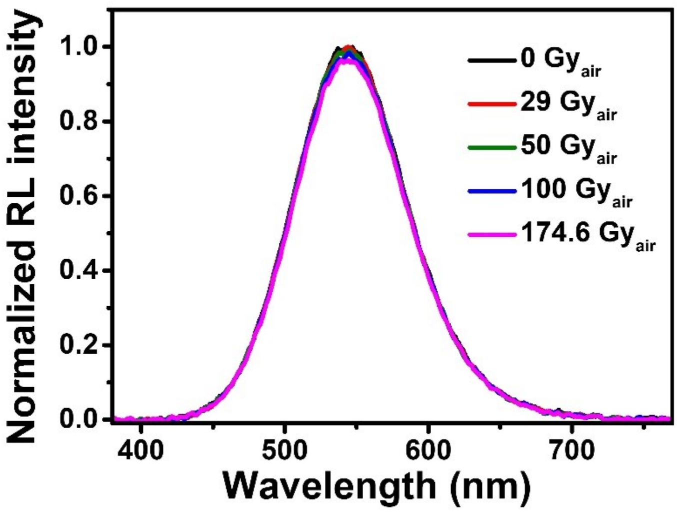

Figure S10. RL spectra of the β-$Cs_3Cu_2Cl_5$ films after being irradiated by various X-ray total dose.

Table S1. Comparison of X-ray irradiation hardness of β-$Cs_3Cu_2Cl_5$, CsI:Tl, and $Cs_2Ag_{0.6}Na_{0.4}InCl_6$:$Yb^{3+}$/$Er^{3+}$/$Bi^{3+}$ (RE-1).

Total X-ray dose [Gy_{air}]		0	13	29	53	Ref.
Normalized RL intensity	β-$Cs_3Cu_2Cl_5$	100%	99.2%	99.1%	98.6%	This work
	CsI:Tl	100%	~97%	~50%	~28%	[1]
	RE-1	100%	71%	60%	49%	[2]

Slanted-edge method:[3]

Firstly, the X-ray images was converted into grey-scale map and the edge spread function (ESF) stands for the grey information along a certain direction. The line spread function (LSF) could be deduced by taking the differential on the edge spread function (ESF), as following:

$$LSF(x) = \frac{dESF(x)}{dx}$$

Where x is the position of pixels, which is defined by following formular:

$$x = \frac{N \cdot d}{\beta}$$

Where N is the ordinal number of the image along a certain direction, d is the pixel size (about 6 μm) of the CMOS sensor in camera and β is the optical magnification.

Modulation Transfer Function (MTF) curve can be deduced by the Fourier transform of the LSF, as following:

$$MTF(v) = F(LSF(x))$$

Where v is the spatial frequency.

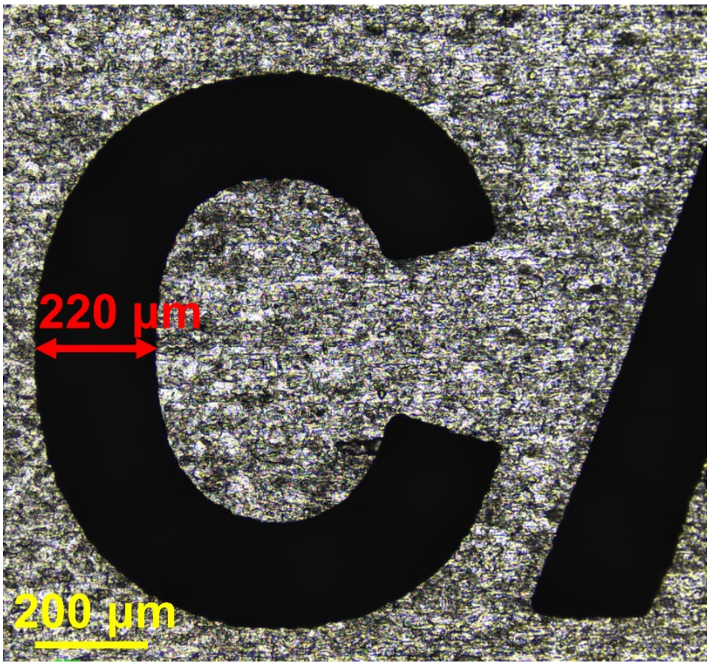

Figure S11. Optical microscope photograph showing the line width of the smallest CAEP letters in the mask.

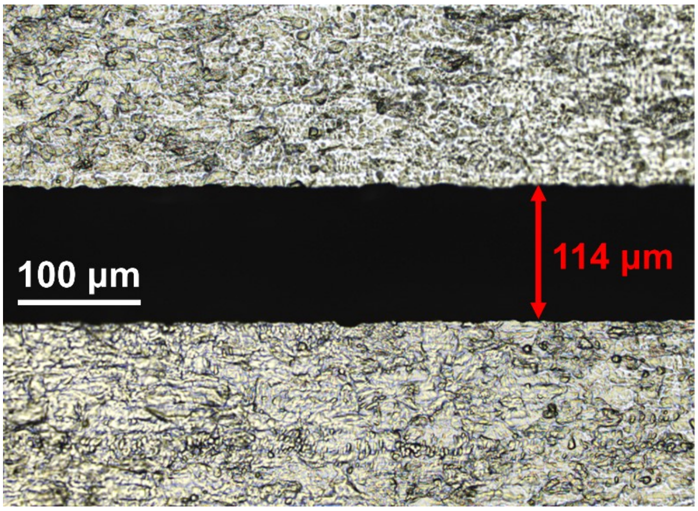

Figure S12. Optical microscope photograph of the finest line in the mask.

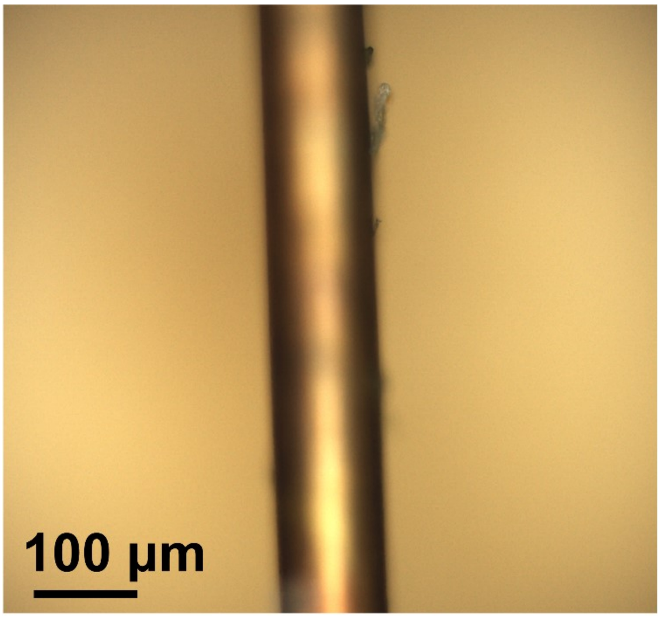

Figure S13. Optical microscope photograph of the copper wire with a diameter of 100 µm.

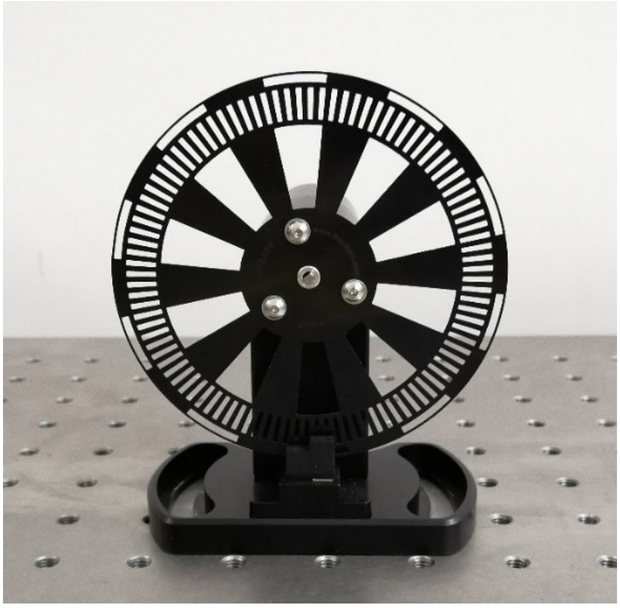

Figure S14. Photograph of the chopper blades.

Reference

[1] Y. Wang, X. Yin, W. Liu, J. Xie, J. Chen, M. A. Silver, D. Sheng, L. Chen, J. Diwu, N. Liu, Z. Chai, T. E. Albrecht-Schmitt, S. Wang, *Angew. Chem., Int. Ed.* **2018**, 57, 7883.

[2] Z. Zeng, B. Huang, X. Wang, L. Lu, Q. Lu, M. Sun, T. Wu, T. Ma, J. Xu, Y. Xu, S. Wang, Y. Du, C.-H. Yan, *Adv. Mater.* **2020**, 32, 2004506.

[3] W. Ma, T. Jiang, Z. Yang, H. Zhang, Y. Su, Z. Chen, X. Chen, Y. Ma, W. Zhu, X. Yu, H. Zhu, J. Qiu, X. Liu, X. Xu, Y. Yang, *Advanced Science* **2021**, 8, 2003728.